

Anomalous spin Josephson effect in spin superconductors

Wen Zeng(曾文) and Rui Shen(沈瑞)
Citation: Chin. Phys. B, 2024, 33 (**3**): 037401. DOI: 10.1088/1674-1056/ad1982
Journal homepage: http://cpb.iphy.ac.cn; http://iopscience.iop.org/cpb

What follows is a list of articles you may be interested in

Photoinduced valley-dependent equal-spin Andreev reflection in Ising superconductor junction

Wei-Tao Lu(卢伟涛), Yue Mao(毛岳), and Qing-Feng Sun(孙庆丰)
Chin. Phys. B, 2023, 32 (**10**): 107403. DOI: 10.1088/1674-1056/aceee6

Asymmetric Fraunhofer pattern in Josephson junctions from heterodimensional superlattice V_5S_8

Juewen Fan(范珏雯), Bingyan Jiang(江丙炎), Jiaji Zhao(赵嘉佶), Ran Bi(毕然), Jiadong Zhou(周家东), Zheng Liu(刘政), Guang Yang(杨光), Jie Shen(沈洁), Fanming Qu(屈凡明), Li Lu(吕力), Ning Kang(康宁), and Xiaosong Wu(吴孝松)
Chin. Phys. B, 2022, 31 (**5**): 057402. DOI: 10.1088/1674-1056/ac5d30

Josephson current in an irradiated Weyl semimetal junction

Han Wang(王含) and Rui Shen(沈瑞)
Chin. Phys. B, 2021, 30 (**7**): 077406. DOI: 10.1088/1674-1056/ac0348

0-π transition induced by the barrier strength in spin superconductor Josephson junctions

Wen Zeng(曾文), Rui Shen(沈瑞)
Chin. Phys. B, 2018, 27 (**9**): 097401. DOI: 10.1088/1674-1056/27/9/097401

Novel 0-π transitions in Josephson junctions between noncentrosymmetric superconductors

Jun-Feng Liu(刘军丰), Huan Zhang(张欢), Jun Wang(汪军)
Chin. Phys. B, 2016, 25 (**9**): 097403. DOI: 10.1088/1674-1056/25/9/097403

RAPID COMMUNICATION

Anomalous spin Josephson effect in spin superconductors

Wen Zeng(曾文)[1,2,†] and Rui Shen(沈瑞)[3,4]

[1] *School of Physics and Electronic Engineering, Jiangsu University, Zhenjiang* 212013, *China*
[2] *Jiangsu Engineering Research Center on Quantum Perception and Intelligent, Detection of Agricultural Information, Zhenjiang* 212013, *China*
[3] *National Laboratory of Solid State Microstructures and School of Physics, Nanjing University, Nanjing* 210093, *China*
[4] *Collaborative Innovation Center of Advanced Microstructures, Nanjing University, Nanjing* 210093, *China*

(Received 7 November 2023; revised manuscript received 27 December 2023; accepted manuscript online 29 December 2023)

The spin superconductor state is the spin-polarized triplet exciton condensate, which can be viewed as a counterpart of the charge superconductor state. As an analogy of the charge Josephson effect, the spin Josephson effect can be generated in the spin superconductor/normal metal/spin superconductor junctions. Here we study the spin supercurrent in the Josephson junctions consisting of two spin superconductors with noncollinear spin polarizations. For the Josephson junctions with out-of-plane spin polarizations, the possible π-state spin supercurrent appears due to the Fermi momentum-splitting Andreev-like reflections at the normal metal/spin superconductor interfaces. For the Josephson junctions with in-plane spin polarizations, the anomalous spin supercurrent appears and is driven by the misorientation angle of the in-plane polarizations. The symmetry analysis shows that the appearance of the anomalous spin Josephson current is possible when the combined symmetry of the spin rotation and the time reversal is broken.

Keywords: tunneling junction, spin supercurrent, 0–π transition, anomalous spin Josephson effect

PACS: 74.50.+r, 73.43.jn **DOI:** 10.1088/1674-1056/ad1982

1. Introduction

The exciton condensates are composed of the electron–hole pairs which are charge neutral while their spin may either be singlet or triplet.[1,2] The key issue to realize the stable exciton condensates is to prevent the electron–hole recombination.[3,4] Many strategies have been proposed to do so, such as the exciton condensates realized in the double-layer systems,[5–8] where two monolayers are spatially separated by an insulator layer. The insulator is supposed to be high enough to prevent the electron–hole recombination. Recently, Sun *et al.*[9,10] suggested that the stable spin-polarized triplet exciton condensates could be realized in the graphene monolayer growing on a ferromagnetic material or under an external magnetic field, where the electron-like spin-up states are below the hole-like spin-down states,[9] which prevents the electron–hole recombination and means the exciton condensates in the ferromagnetic graphene system are stable. These stable exciton condensates are termed as the spin superconductor states.[9,10] Analogous to the Andreev reflection in charge superconductors,[11–16] Lv *et al.*[17] studied the Andreev-like reflection in the normal metal/spin superconductor (NS) junctions based on the ferromagnetic graphene, where an incident spin-up electron is reflected as a spin-down electron and the spin $2\times(\hbar/2)$ is injected into the spin superconductor. This spin-flipped Andreev-like reflection leads to the spin current when a spin voltage is applied across the junction.

Inspired by this, in this paper we investigate the spin Josephson effect in the device consisting of two weakly coupled spin superconductors with noncollinear spin polarizations. Both the out-of-plane spin polarization configuration and the in-plane spin polarization configuration are considered, as shown in Figs. 1(a) and 1(b), respectively. We show that the repeated spin-flipped Andreev-like reflections at the NS interfaces lead to the Andreev-like bound states, which are responsible for the dissipationless spin supercurrent. This spin supercurrent is driven by the macroscopic phase difference ϕ_s, which origins from a spin current flowing through the junction under the drive of an external device or from a variation of an external electric field thread the ring junction device.[9] As the condensed electron–hole pairs in spin superconductors are charge neutral, the charge current in our model is zero. For the Josephson junctions with out-of-plane spin polarizations, the possible π-state spin supercurrent can be generated due to the Fermi momentum-splitting Andreev-like reflections at the NS interfaces. The anomalous spin supercurrent is absent and the phase of the spin supercurrent is determined by the Fermi level and the junction length. For the Josephson junctions with in-plane spin polarizations, the misorientation angle of the in-plane polarizations acts as an effective superconducting phase, leading to a finite spin superconducting current at zero phase difference, which is termed as the anomalous spin Josephson effect. Furthermore, the symmetry analysis shows that the appearance of the anomalous spin Josephson current is possible when the combined symmetry of the spin rotation and the time

[†]Corresponding author. E-mail: zeng@ujs.edu.cn

© 2024 Chinese Physical Society and IOP Publishing Ltd

reversal is broken.

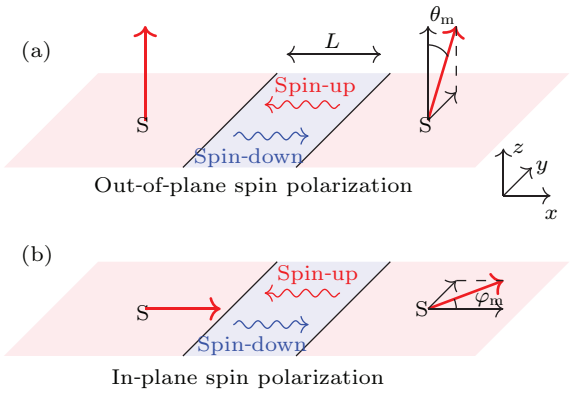


Fig. 1. Schematic of the spin Josephson junctions with the length of the normal region being L. The red arrows denote the directions of the spin polarization of the triplet exciton condensates. The red and blue wavy lines denote the left-propagating spin-up electron and the right-propagating spin-down electron, respectively. (a) The spin Josephson junction with out-of-plane spin polarization. The spin polarization of the triplet exciton condensate in the left spin superconductor is along the z axis and the spin polarization of the triplet exciton condensate in the right spin superconductor lies in the y–z plane with the polar angle θ_m. (b) The spin Josephson junction with in-plane spin polarization. The spin polarization of the triplet exciton condensate in the left spin superconductor is along the x axis and the spin polarization of the triplet exciton condensate in the right spin superconductor lies in the x–y plane with the azimuthal angle φ_m.

The remainder of the paper is organized as follows. The model Hamiltonian and the scattering approach are explained in detail in Section 2. The numerical results and discussion are presented in Section 3. Finally, we conclude in Section 4.

2. Model and formulation

2.1. Model Hamiltonian

The model Hamiltonian for the spin superconductor with the spin polarization along z axis is given by[9,17]

$$\mathcal{H}_S = \begin{pmatrix} \mathcal{H}_0 + M & \Delta_s \tau_z \\ \Delta_s^* \tau_z & \mathcal{H}_0 - M \end{pmatrix}, \tag{1}$$

where M is the exchange split energy induced by the proximity to an insulating ferromagnetic layer,[18,19] and Δ_s is the spin superconducting pair potential induced by the electron–hole Coulomb attraction interaction.[9] The single-particle Hamiltonian $\mathcal{H}_0$ reads[20,21]

$$\mathcal{H}_0 = \hbar v_F (k_x \tau_x + \eta k_y \tau_y) - \mu, \tag{2}$$

where $\eta = +\,(-)$ for K (K') valley, v_F is the Fermi velocity, μ is the Fermi energy, k_x (k_y) is the wave vector in the x (y) direction, and $\tau_{x,y,z}$ is the Pauli matrix in the pseudospin space. For the spin superconductor with the spin polarization

$$\boldsymbol{n} = (\sin\theta_m \cos\varphi_m, \sin\theta_m \sin\varphi_m, \cos\theta_m), \tag{3}$$

the Hamiltonian is given by

$$\mathcal{H}_S(\boldsymbol{n}) = \mathcal{R}_{\boldsymbol{n}} \mathcal{H}_S \mathcal{R}_{\boldsymbol{n}}^{\dagger}, \tag{4}$$

where the spin rotation matrix is given by

$$\mathcal{R}_{\boldsymbol{n}} = \begin{pmatrix} \cos\left(\frac{\theta_m}{2}\right)\tau_0 & e^{-i\varphi_m}\sin\left(\frac{\theta_m}{2}\right)\tau_0 \\ e^{i\varphi_m}\sin\left(\frac{\theta_m}{2}\right)\tau_0 & \cos\left(\frac{\theta_m}{2}\right)\tau_0 \end{pmatrix}, \tag{5}$$

with τ_0 being the identity matrix in the pseudospin space, θ_m and φ_m being the polar angle and the azimuthal angle, respectively.

We consider the spin superconductor/normal metal/spin superconductor junctions in the x–y plane, where the spin polarizations of the two spin superconducting regions are non-collinear, as schematically shown in Fig. 1. The junction is described by the Bogoliubov–de Gennes (BdG) Hamiltonian,[22] which is given by

$$\mathcal{H}_{BdG} = \mathcal{H}_L + \mathcal{H}_N + \mathcal{H}_R, \tag{6}$$

where $\mathcal{H}_L = \mathcal{H}_S(\boldsymbol{n}_L)\Theta(-x)$, $\mathcal{H}_R = \mathcal{H}_S(\boldsymbol{n}_R)\Theta(x-L)$ and $\mathcal{H}_N = \mathcal{H}_S|_{\Delta\to 0}\Theta(x)\Theta(L-x)$ with $\boldsymbol{n}_{L(R)}$ being the spin polarization for the left (right) spin superconductor and $\Theta(x)$ being the Heaviside step function. The superconducting pair potential is $\Delta_s = \Delta e^{-i\phi_s/2}$ for $x<0$ and $\Delta_s = \Delta e^{i\phi_s/2}$ for $x>L$, where ϕ_s is the phase difference across the junction.

2.2. Transfer matrix

The scattering states of the spin superconductor with spin polarization $\boldsymbol{n}$ can be obtained by

$$\psi_{\varsigma\rho}^{(\boldsymbol{n})} = \mathcal{R}_n \begin{pmatrix} e^{i\frac{\phi_s}{2}} e^{-i\frac{\varsigma\rho\beta_\rho}{2}} e^{i\frac{\rho\gamma}{2}} \\ \varsigma\rho\, e^{i\frac{\phi_s}{2}} e^{i\frac{\varsigma\rho\beta_\rho}{2}} e^{i\frac{\rho\gamma}{2}} \\ e^{-i\frac{\phi_s}{2}} e^{-i\frac{\varsigma\rho\beta_\rho}{2}} e^{-i\frac{\rho\gamma}{2}} \\ \varsigma\rho\, e^{-i\frac{\phi_s}{2}} e^{i\frac{\varsigma\rho\beta_\rho}{2}} e^{-i\frac{\rho\gamma}{2}} \end{pmatrix} \times e^{i\varsigma\rho k_\rho x + i k_y y}, \tag{7}$$

where $\varsigma = +\,(-)$ for the right (left) propagating states, $\rho = +\,(-)$ for the electron-like (hole-like) quasiparticles, the longitudinal wave vector is $k_\rho = \sqrt{(-M + i\rho\sqrt{\Delta^2 - E^2})^2/\hbar^2 v_F^2 - k_y^2}$ with k_y and E being the conserved transverse wave vector and the incident energy, respectively, $\beta_\rho = \arctan(k_y/k_\rho)$, $\gamma = \arccos(E/\Delta)$ for $E<\Delta$ and $\gamma = -i\,\mathrm{arccosh}(E/\Delta)$ for $E>\Delta$.

Due to the spin-flipped Andreev-like reflection at the NS interface,[17] the incident and reflected states are connected by $\psi_{\bar\sigma} = \mathcal{S}\psi_\sigma$ with $\mathcal{S}$ being the transfer matrix, ψ_σ ($\psi_{\bar\sigma}$) being the spin-σ (spin-$\bar\sigma$) component in Eq. (7) ($\bar\sigma \equiv -\sigma$). The transfer matrices at the left and right interfaces can be directly obtained by matching the left and right propagating states in Eq. (7), respectively, which are given by

$$\mathcal{S}_\nu = \frac{e^{i\varphi_\nu}\sin\left(\frac{\theta_\nu}{2}\right) + \cos\left(\frac{\theta_\nu}{2}\right)\mathcal{S}_\nu^{(0)}}{\cos\left(\frac{\theta_\nu}{2}\right) + e^{-i\varphi_\nu}\sin\left(\frac{\theta_\nu}{2}\right)\mathcal{S}_\nu^{(0)}}, \tag{8}$$

with $\nu = +\ (-)$ for the left (right) interface. $\mathcal{S}_\nu^{(0)}$ is the Andreev-like transfer matrix for $\theta_{\rm m} = 0$, which is given by

$$\mathcal{S}_\nu^{(0)} = {\rm e}^{-{\rm i}\phi_\nu} \begin{pmatrix} \cos\gamma & -{\rm i}\nu\sin\gamma \\ {\rm i}\nu\sin\gamma & -\cos\gamma \end{pmatrix}. \tag{9}$$

In the normal region, the electron transfer matrix is readily obtained by[23]

$$\mathcal{M} = \Lambda\, {\rm e}^{{\rm i}kL\tau_z}\Lambda, \tag{10}$$

$$\Lambda = \frac{1}{\sqrt{2\cos\alpha}} \begin{pmatrix} {\rm e}^{-{\rm i}\alpha/2} & {\rm e}^{{\rm i}\alpha/2} \\ {\rm e}^{{\rm i}\alpha/2} & -{\rm e}^{-{\rm i}\alpha/2} \end{pmatrix}, \tag{11}$$

where $k = k_{\rm F}\cos\alpha$ is the longitudinal wave vector in the normal region with $k_{\rm F} = \mu/(\hbar v_{\rm F})$ being the Fermi wave vector and $\alpha = \arcsin(\hbar v_{\rm F} k_y/\mu) \in [-\pi/2, \pi/2]$ is the incident angle.

The total spin Josephson current density can be obtained by[24,25]

$$j = -k_{\rm B}T \sum_{n,k_y} \frac{\rm d}{{\rm d}\phi_{\rm s}} \ln\det\left(1 - \mathcal{M}^{-1}\mathcal{S}_+^{-1}\mathcal{M}\mathcal{S}_-\right), \tag{12}$$

where $k_{\rm B}$ is the Boltzmann constant, T is the temperature, and the energy variable in the determinant is replaced by ${\rm i}\omega_n$ with $\omega_n = (2n+1)\pi k_{\rm B}T$ ($n \in \mathbb{Z}$).

3. Results

In the following calculations, we set $\Delta = 1$ meV as the energy unit. The superconducting coherence length is $\xi = \hbar v_{\rm F}/\Delta \approx 360$ nm, which is set as the length unit.

3.1. Josephson junction with out-of-plane spin polarization

The Josephson junction with the out-of-plane spin polarization is schematically shown in Fig. 1(a), where the spin polarization in the left superconducting region is along the z axis and the spin polarization in the right superconducting region lies in the y–z plane with the polar angle $\theta_{\rm m}$. The Andreev-like transfer matrices at the NS interfaces are given by

$$\mathcal{S}_\nu = \frac{1}{\cos\theta_\nu\cos\phi_\nu + {\rm i}\sin\phi_\nu} \times \begin{pmatrix} \sin\theta_\nu\cos\phi_\nu + \cos\gamma & -{\rm i}\sin\gamma \\ {\rm i}\sin\gamma & \sin\theta_\nu\cos\phi_\nu - \cos\gamma \end{pmatrix}, \tag{13}$$

where $\nu = +\ (-)$ for the right (left) interface, $\theta_+ = \theta_{\rm m}$, $\theta_- = 0$, and $\phi_\pm = \pm\phi_{\rm s}/2$. The Andreev-like bound states can be found from the same determinant in Eq. (12), which are given by

$$\det\left(1 - \mathcal{M}^{-1}\mathcal{S}_+^{-1}\mathcal{M}\mathcal{S}_-\right) = 0, \tag{14}$$

leading to the Andreev-like levels

$$\left|\frac{E_\pm}{\Delta}\right| = \sqrt{\frac{Y^2 - 2XZ \pm \sqrt{Y^2 - 4Y^2Z(X+Z)}}{2(X^2+Y^2)}},$$
$$X = 2\sin^2\alpha - (3+\cos 2\alpha)\cos(2kL),$$
$$Y = -4\cos\alpha\sin(2kL),$$
$$Z = \cos^2\alpha\left(\cos\phi_{\rm s} + \cos\theta_{\rm m}\cos\phi_{\rm s} + \cos\theta_{\rm m} + 2\cos(2kL) - 1\right). \tag{15}$$

With the help of Eq. (12), the spin Josephson current density at $T = 0$ K can be obtained by the $\phi_{\rm s}$-dependent Andreev-like levels

$$j(\phi_{\rm s}) = -\sum_{\ell=\pm}\int \frac{\mu W}{2\pi\hbar v_{\rm F}} \frac{{\rm d}E_\ell}{{\rm d}\phi_{\rm s}} \cos\alpha\, {\rm d}\alpha, \tag{16}$$

where E_ℓ is the positive root of Eq. (15) and W is the width of the junction.

The supercurrent–phase relations at different $\theta_{\rm m}$ are shown in Fig. 2(a) for $k_{\rm F}L = 0.1$. The spin Josephson current decreases with the increase of $\theta_{\rm m}$, and drops to zero when the spin polarizations in the left and right superconducting regions are antiparallel, i.e., $\theta_{\rm m} = \pi$. In this antiparallel configuration, the spin polarizations of the spin-triplet electron–hole condensations in the left and right spin superconductors are opposite, the Andreev-like process between two NS interfaces can not form a closed loop. Consequently, the $\phi_{\rm s}$-dependent Andreev-like levels are absent, leading to the zero spin supercurrent.

For $k_{\rm F}L = 2$, the spin supercurrent is reversed and the π-state Josephson junction appears, as shown in Fig. 2(b). This 0–π phase transition is attributed to the Fermi-momentum splitting Andreev-like reflections at the NS interfaces. At the Fermi surface, the right-propagating spin-up electron with the wave vector $k_{\rm F}$ is converted into a left-propagating spin-down electron with the wave vector $-k_{\rm F}$ due to the Andreev-like reflection, leading to the wave vector difference $\Delta k = 2k_{\rm F}$. An additional phase shift $2k_{\rm F}L$ is accumulated in a closed Andreev loop. The total scattering phase acquired by the electrons in this closed Andreev loop is $2k_{\rm F}L \pm \phi_{\rm s} - 2\arccos(E/\Delta)$,[26] which should be quantized according to the quasiclassical Bohr–Sommerfeld quantization condition,[27,28] i.e., $2k_{\rm F}L \pm \phi_{\rm s} - 2\arccos(E/\Delta) = 2\pi n$ ($n \in \mathbb{Z}$). Consequently, the state of the junction can be controlled by the phase factor $\cos(k_{\rm F}L)$. The spin supercurrent can be expressed as $j \propto \cos(k_{\rm F}L)\sin\phi_{\rm s}$. For $2n\pi + \pi/2 < k_{\rm F}L < 2n\pi + 3\pi/2$, the spin supercurrent is reversed.

The critical spin current defined by $j_{\rm c} = \max|j(\phi_{\rm s})|$ as a function of the junction length L is shown in Fig. 2(c). Due to the additional phase $k_{\rm F}L$, the critical spin current is proportional to $\cos(k_{\rm F}L)$, which exhibits an oscillation behavior as the junction length increases. For $\mu = 0.5\Delta$ in Fig. 2(c), the oscillation period can be estimated as $T_L = \pi/k_{\rm F} = 2\pi\xi$. The critical spin current as a function of the polar angle $\theta_{\rm m}$ is shown in Fig. 2(d). The $\theta_{\rm m}$-dependent critical spin current is symmetric due to the rotation symmetry, i.e., $j_{\rm c}(\theta_{\rm m}) = j_{\rm c}(-\theta_{\rm m})$. The critical spin current reaches its maximum value at $\theta_{\rm m} = 0$ and becomes zero at $\theta_{\rm m} = \pm\pi$.

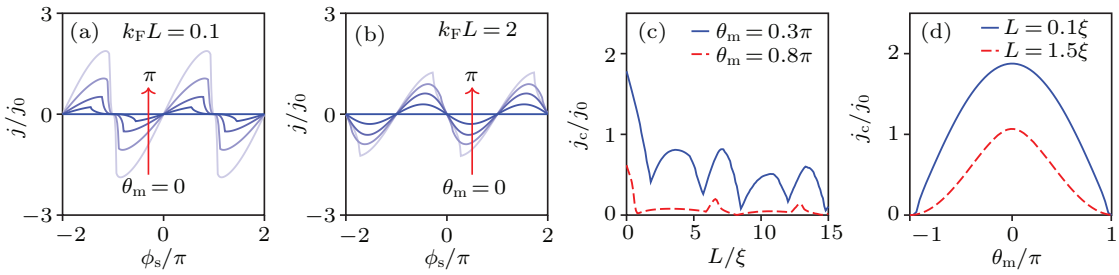


Fig. 2. (a), (b) The current–phase relation for the Josephson junctions with the out-of-plane spin polarization. The red arrows indicate the curves with the increasing deviation of the relative angles θ_m, which change from 0 to π with a step of $\pi/4$. (c) The critical spin Josephson current density j_c as a function of L for $\theta_m = 0.3\pi$ (solid) and $\theta_m = 0.8\pi$ (dashed). The Fermi level is $\mu = 0.5\Delta$. (d) The critical spin Josephson current density j_c as a function of θ_m for $L = 0.1\xi$ (solid) and $L = 1.5\xi$ (dashed). Both j and j_c are renormalized by $j_0 = \mu\Delta W/(2\pi\hbar v_F)$.

3.2. Josephson junction with in-plane spin polarization

The Josephson junction with in-plane spin polarization is schematically shown in Fig. 1(b), where the spin polarization in the left superconducting region is along the x axis and the spin polarization in the right superconducting region lies in the x–y plane with the azimuthal angle φ_m. The Andreev-like transfer matrices are given by

$$\mathcal{S}_\nu = \frac{-\mathrm{i}\,\mathrm{e}^{\mathrm{i}\varphi_\nu}}{\sin(\varphi_\nu+\phi_\nu)} \times \begin{pmatrix} \cos(\varphi_\nu+\phi_\nu)+\cos\gamma & -\mathrm{i}\sin\gamma \\ \mathrm{i}\sin\gamma & \cos(\varphi_\nu+\phi_\nu)-\cos\gamma \end{pmatrix}, \quad (17)$$

where $\nu = +\ (-)$ for the right (left) interface, $\varphi_+ = \varphi_m$, $\varphi_- = 0$, and $\phi_\pm = \pm\phi_s/2$. The Andreev-like levels are given by

$$\begin{aligned} \left|\frac{E_\pm}{\Delta}\right| &= \sqrt{\frac{\bar{Y}^2 - 2\bar{X}\bar{Z} \pm \sqrt{\bar{Y}^2 - 4\bar{Y}^2\bar{Z}(\bar{X}+\bar{Z})}}{2(\bar{X}^2+\bar{Y}^2)}}, \\ \bar{X} &= 8(3\cos(2kL) + 2\cos 2\alpha\cos^2(kL) - 1), \\ \bar{Y} &= 32\cos\alpha\sin(2kL), \\ \bar{Z} &= -4\cos^2\alpha\big(2\cos\varphi_m - \cos 2\varphi_m + \cos\phi_s \\ &\quad + 2\cos(\varphi_m+\phi_s) + \cos(2\varphi_m+\phi_s) \\ &\quad + 4\cos(2kL) - 1\big). \end{aligned} \quad (18)$$

The zero-temperature spin Josephson current obtained by Eq. (16) is shown in Fig. 3(a) at $k_FL = 0.1$. Due to the spin rotation symmetry, the spin supercurrent for the Josephson junctions with parallel in-plane spin polarization ($\varphi_m = 0$) is the same as that for the Josephson junctions with parallel out-of-plane spin polarization ($\theta_m = 0$). For the antiparallel in-plane polarization ($\varphi_m = \pi$), the spin Josephson current is absent due to the absence of the ϕ_s-dependent Andreev-like levels.

For $\varphi_m \neq 0$ and $\varphi_m \neq \pi$, the anomalous spin Josephson current $j|_{\phi_s=0}$ appears, as shown in Fig. 3(a). For simplicity, we present the spin Josephson current for the one-dimensional (1D) case with $k_y = 0$

$$j_{1D} \propto \cos(k_FL)\cos^2\left(\frac{\varphi_m}{2}\right)\sin(\phi_s+\varphi_m), \quad (19)$$

which can imply the qualitative properties of the two-dimensional Josephson junctions. Equation (19) shows that the anomalous spin Josephson current at $\phi_s = 0$ is proportional to $\cos(k_FL)\cos^2(\varphi_m/2)\sin\varphi_m$. The spin Josephson current can be reversed by the additional phase factor $\cos(k_FL)$. For $k_FL = 2$, the reversed spin Josephson current obtained from Eq. (16) is shown in Fig. 3(b).

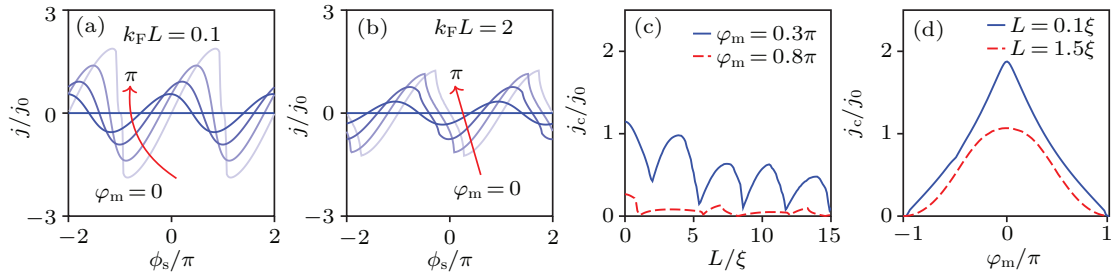


Fig. 3. (a), (b) The current–phase relation for the Josephson junctions with the in-plane spin polarization. The red arrows indicate the curves with the increasing deviation of the relative angles φ_m, which change from 0 to π with a step of $\pi/4$. (c) The critical spin Josephson current density j_c as a function of L for $\varphi_m = 0.3\pi$ (solid) and $\varphi_m = 0.8\pi$ (dashed). The Fermi level is $\mu = 0.5\Delta$. (d) The critical spin Josephson current density j_c as a function of θ_m for $L = 0.1\xi$ (solid) and $L = 1.5\xi$ (dashed). Both j and j_c are renormalized by $j_0 = \mu\Delta W/(2\pi\hbar v_F)$.

The critical spin currents j_c as a function of the junction length L and the azimuthal angle φ_m are shown in Figs. 3(c) and 3(d), respectively. The L-dependent oscillation is determined by the additional phase factor $\cos(k_FL)$ due to the Fermi-moment splitting. For a fixed L, the φ_m-resolved j_c is symmetric, as shown in Fig. 3(d).

The anomalous spin Josephson current $j|_{\phi_s=0}$ as a function of L is shown in Fig. 4(a). For $\varphi_m = 0$ and $\varphi_m = \pi$, the

anomalous Josephson effect is absent. For $\varphi_m \neq 0$ and $\varphi_m \neq \pi$, $j|_{\phi_s=0}$ oscillates with the increase of L and has the same oscillation period as j_c. For $\mu = \Delta$ in Fig. 4(a), the oscillation period is about $\pi\xi$. $j|_{\phi_s=0}$ as a function of φ_m is shown in Fig. 4(b). The φ_m-resolved anomalous spin Josephson current is asymmetric and satisfies the relation

$$j|_{\phi_s=0}(\varphi_m) = -j|_{\phi_s=0}(-\varphi_m), \tag{20}$$

due to the symmetry of the BdG Hamiltonian, which is explained in detail in Subsection 3.3.

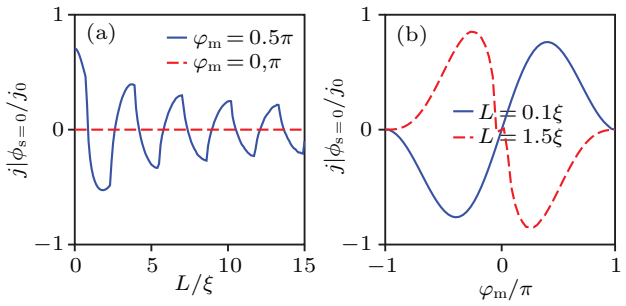


Fig. 4. (a) The anomalous spin Josephson current density $j|_{\phi_s=0}$ as a function of L for $\varphi_m = 0.5\pi$ (solid) and $\varphi_m = 0, \pi$ (dashed). The Fermi level is $\mu = \Delta$. (b) The anomalous spin Josephson current $j|_{\phi_s=0}$ as a function of φ_m for $L_m = 0.1\xi$ (solid) and $L = 1.5\xi$ (dashed). $j|_{\phi_s=0}$ is renormalized by $j_0 = \mu\Delta W/(2\pi\hbar v_F)$.

3.3. Symmetry analysis

The Hamiltonian of the spin superconductor with out-of-plane spin polarization can be written as

$$\mathcal{H}_S^\eta = h_\eta(k) + \mathcal{H}'(\phi_s, \theta_m), \tag{21}$$

where $\eta = \pm$ is the valley index, the k-dependent term $h_\eta(k) = \hbar v_F(k_x\tau_x + \eta k_y\tau_y)$ is the Hamiltonian of the pristine graphene for the η valley and the k-independent term is given by

$$\begin{aligned}\mathcal{H}'(\phi_s, \theta_m) =\ & M\cos\theta_m\sigma_z\tau_0 + M\sin\theta_m\sigma_x\tau_0 \\ & + \Delta\cos\theta_m\cos\phi_s\sigma_x\tau_z + \Delta\sin\theta_m\cos\phi_s\sigma_z\tau_z \\ & - \Delta\sin\phi_s\sigma_y\tau_z.\end{aligned} \tag{22}$$

Under the time-reversal transformation, the Hamiltonian of the pristine graphene remains unchanged

$$\begin{aligned}h_\eta(k) &\to \mathcal{T}h_{\bar\eta}(-k)\mathcal{T}^{-1} \\ &= \hbar v_F(k_x\tau_x + \eta k_y\tau_y) \\ &= h_\eta(k),\end{aligned} \tag{23}$$

where $\bar\eta = -\eta$, $\mathcal{T} = i\sigma_y\tau_z\mathcal{C}$ is the time-reversal operator with $\mathcal{C}$ being the complex conjugation. For the k-independent Hamiltonian $\mathcal{H}'(\phi_s, \theta_m)$, considering the combined symmetry $\mathcal{P} = \sigma_y\mathcal{T}$ with σ_y being the spin rotation symmetry and $\mathcal{T}$ being the time-reversal symmetry, one finds that

$$\mathcal{P}\mathcal{H}'(\phi_s, \theta_m)\mathcal{P}^{-1} = \mathcal{H}'(-\phi_s, \theta_m). \tag{24}$$

Due to the spin degeneracy in pristine graphene, $h_\eta(k)$ remains unchanged under $\mathcal{P}$. Consequently, with the help of Eq. (6), the BdG Hamiltonian for the Josephson junctions with the out-of-plane spin polarization holds the relation

$$\mathcal{P}\mathcal{H}_{BdG}(\phi_s, \theta_m)\mathcal{P}^{-1} = \mathcal{H}_{BdG}(-\phi_s, \theta_m). \tag{25}$$

The spin Josephson current density can be obtained via the thermodynamic relation[29,30]

$$j(\phi_s) = -k_B T\partial_{\phi_s}\ln\mathrm{Tr}[e^{-\mathcal{H}_{BdG}(\phi_s)/k_B T}]. \tag{26}$$

By substituting Eq. (25) into Eq. (26), one finds that the spin Josephson current holds the relation

$$j(\phi_s, \theta_m) = -j(-\phi_s, \theta_m), \tag{27}$$

leading to the absence of the anomalous spin Josephson current, i.e., $j|_{\phi_s=0} = 0$.

For the spin superconductor with in-plane spin polarization, the Hamiltonian can be written as

$$\mathcal{H}_S^\eta = h_\eta(k) + \mathcal{H}''(\phi_s, \varphi_m), \tag{28}$$

with

$$\begin{aligned}\mathcal{H}''(\phi_s, \varphi_m) =\ & M\cos\varphi_m\sigma_x\tau_0 + M\sin\varphi_m\sigma_y\tau_0 \\ & - \Delta\sin(\varphi_m + \phi_s)\cos\varphi_m\sigma_y\tau_z \\ & + \Delta\sin(\varphi_m + \phi_s)\sin\varphi_m\sigma_x\tau_z \\ & - \Delta\cos(\varphi_m + \phi_s)\sigma_z\tau_z.\end{aligned} \tag{29}$$

The symmetry $\mathcal{P}$ is broken and the BdG Hamiltonian holds the relation

$$\mathcal{P}\mathcal{H}_{BdG}(\phi_s, \varphi_m)\mathcal{P}^{-1} = \mathcal{H}_{BdG}(-\phi_s, -\varphi_m). \tag{30}$$

With the help of Eq. (26), one finds that the spin Josephson current holds the relation

$$j(\phi_s, \varphi_m) = -j(-\phi_s, -\varphi_m), \tag{31}$$

leading to the presence of the anomalous spin Josephson current. The anomalous spin Josephson current is an odd function of φ_m satisfying $j|_{\phi_s=0}(\varphi_m) = -j|_{\phi_s=0}(-\varphi_m)$, as shown in Fig. 4(b).

In fact, the anomalous Josephson effect is possible when the symmetries $\mathcal{T}$, $\mathcal{D}$ and $\mathcal{P}$ are all broken,[31,32] where $\mathcal{D} = \sigma_y R_{xz}\mathcal{T}$ is another combined symmetry with R_{xz} being the mirror reflection about the x–z plane. We note that the symmetries $\mathcal{T}$ and $\mathcal{D}$ are always broken in our model for both the out-of-plane spin polarization and the in-plane spin polarization. The combined symmetry $\mathcal{P}$ plays a key role in our model: For the Josephson junction with out-of-plane spin polarization, the absence of the anomalous spin Josephson current ($j|_{\phi_s=0} = 0$) is protected by $\mathcal{P}$. For the Josephson junction with in-plane spin polarization, the breaking of $\mathcal{P}$ leads to the presence of the anomalous spin Josephson current.

4. Conclusions

To conclude, we theoretically investigate the spin Josephson effect in the spin superconductor/normal metal/spin superconductor junctions, where the spin polarizations of the left and right spin superconducting regions are noncollinear. For the Josephson junctions with out-of-plane spin polarization, the possible π-state spin supercurrent can be generated due to the Fermi momentum-splitting Andreev-like reflection at the normal metal/spin superconductor interface. For the Josephson junctions with in-plane spin polarization, the anomalous spin supercurrent appears and is driven by the misorientation angle of the in-plane spin polarization. The symmetry analysis shows that the appearance of the anomalous spin Josephson current is possible when the combined symmetry of the spin rotation and the time reversal is broken.

Acknowledgement

Project supported by the National Key R&D Program of China (Grant No. 2022YFA1403601).

References

[1] Jiang Z, Lou W, Liu Y, Li Y, Song H, Chang K, Duan W and Zhang S 2020 *Phys. Rev. Lett.* **124** 166401
[2] Zhang C, Zhang W, Jia Y and Zhang Z 2021 *Phys. Rev. B* **104** 195309
[3] Tachiya M and Seki K 2010 *Phys. Rev. B* **82** 085201
[4] Blom p, Jong M D and Breedijk S 1997 *Appl. Phys. Lett.* **71** 930
[5] Lozovik Y and Yudson V 1976 *Solid State Communications* **19** 391
[6] Zhang C H and Joglekar Y N 2008 *Phys. Rev. B* **77** 233405
[7] Seradjeh B, Weber H and Franz M 2008 *Phys. Rev. Lett.* **101** 246404
[8] Mink M P, Stoof H T C, Duine R A and MacDonald A H 2011 *Phys. Rev. B* **84** 155409
[9] Sun Q F, Jiang Z T, Yu Y and Xie X C 2011 *Phys. Rev. B* **84** 214501
[10] Sun Q F and Xie X C 2013 *Phys. Rev. B* **87** 245427
[11] Pannetier B and Courtois H 2000 *Journal of Low Temperature Physics* **118** 599
[12] Upadhyay S K, Palanisami A, Louie R N and Buhrman R A 1998 *Phys. Rev. Lett.* **81** 3247
[13] Jong M J M D and Beenakker C W J 1995 *Phys. Rev. Lett.* **73** 1657
[14] Law K T, Lee P A and Ng T K 2009 *Phys. Rev. Lett.* **103** 237001
[15] Russo S, Kroug M, Klapwijk T M and Morpurgo A F 2005 *Phys. Rev. Lett.* **95** 027002
[16] Zeng W and Shen R 2002 *Phys. Rev.B* **106** 094503
[17] Lv P, Guo A M, Li H, Liu C, Xie X C and Sun Q F 2017 *Phys. Rev.B* **95** 104516
[18] Uchida M, Koretsune T, Sato S, Kriener M, Nakazawa Y, Nishi-haya S,Taguchi Y, Arita R and Kawasaki M 2019 *Phys. Rev. B* **100** 245148
[19] Bouhadida F, Mandhour L and Charfi-Kaddour S 2020 *Phys. Rev. B* **102** 075443
[20] Beenakker C W J 2008 *Rev. Mod. Phys.* **80** 1337
[21] Beenakker C W J 2006 *Phys. Rev. Lett.* **97** 067007
[22] Gennes P G D *Superconductivity of metals and alloys* (Boca Raton: CRC Press)
[23] Titov M and Beenakker C W J 2006 *Phys. Rev. B* **74** 041401(R)
[24] Hagymasi I, Kormanyos A and Cserti J 2010 *Phys. Rev. B* **82** 134516
[25] Brouwer P and Beenakker C W J 1997 *Chaos, Solitons & Fractals* **7–8** 1249
[26] Kashiwaya S and Tanaka Y 2000 *Reports on Progress in Physics* **10** 63
[27] Floyd E R 1982 *Phys. Rev. D* **25** 1547
[28] Konotop V V and Kevrekidis P G 2003 *Phys. Rev. Lett.* **91** 230402
[29] Bardeen J, Kummel R, Jacobs A E and Tewordt L 1969 *Phys. Rev.* **187** 556
[30] Beenakker C W J 1992 *Phys. Rev. Lett.* **67** 3836
[31] Liu J F and Chan K S 2010 *Phys. Rev. Lett.* **82** 125305
[32] Rasmussen A, Danon J, Suominen H, Nichele F, Kjaergaard M and Flensberg K 2016 *Phys. Rev. B* **93** 155406